Light scattering studies of ZnSe/GaAs heterostructures

H. Talaat, L. Elissa, and S. Negm
Department of Physics, Faculty of Science, Ain Shams University, Cairo, Egypt

E. Burstein, M. S. Yeganeh, and A. G. Yodh
Department of Physics, University of Pennsylvania, Philadelphia, Pennsylvania 19104

(Received 16 March 1994; accepted 9 April 1994)

Raman studies using the allowed and the forbidden longitudinal optical (LO) Fröhlich interactions are employed to investigate the heterostructure of ZnSe/GaAs as a counterpart to three-photon mixing or second harmonic generation studies. Our samples are an undoped ZnSe/GaAs (001) heterojunction with a ZnSe overlayer varying from 50 to 5000 Å. The scattering intensities for the allowed and the forbidden LO interactions at both resonant and nonresonant incident frequencies for ZnSe are investigated. The nonresonant forbidden LO phonon shows the effect previously observed for the pseudomorphic region of ZnSe thickness as well as for thicker films. The allowed LO intensities show a clear interference effect similar to recent interference effects observed in second harmonic generation for identical ZnSe/GaAs heterostructures. At resonant incident frequency in ZnSe, forbidden LO phonon scattering shows strong enhancement and is an order of magnitude larger than the allowed scattering due to wave-vector-dependent scattering in ZnSe.

I. INTRODUCTION

Heterostructure systems continue to attract great interest, both in the linear light scattering studies [e.g., photoluminescence[1] (PL) and electroreflectance[2] (ER)] and the nonlinear light scattering studies (e.g., three-wave mixing[3–8] (3WM): Raman scattering[9–16] (RS) and second harmonic generation[3,4,17] (SHG)]. In particular, the heterostructure ZnSe/GaAs received further attention recently due to the demonstration of laser action in ZnSe near its optical band-gap energy of 2.67 eV.[17] Thin ZnSe layers grow pseudomorphically on GaAs and then abruptly relax, leaving dislocations and point defects at the buried interface. Charge traps are also believed to exist at the interface; however, their nature and origin are still under investigation.[17] Because of selection rules that relate the symmetry characteristics of the excitation to the polarization properties of the photons, both Fröhlich LO phonon Raman scattering and SHG are powerful probes to investigate the bulk of the material,[9–16,3–8,17] and since both are intrinsically sensitive to interfaces, they have also proven to be powerful tools in surface diagnostics.[11–16]

In a Raman study of the ZnSe/GaAs heterostructure, Olego[11–13] investigated the changes in the surface properties (e.g., surface barrier height) induced by varying thicknesses of epitaxially grown ZnSe on the (001) surface of n^- and p^+ doped GaAs using a mixed polarization configuration $z(x+y,x+y)\bar{z}$, thus allowing both bulk (LO-plasmon coupled modes) and surface (field-induced Franz-Keldysh LO modes) to be observed simultaneously. On the other hand, Yeganeh *et al.*[17] used three-photon mixing (3PM) spectroscopy and SHG to probe the interfacial electronic structure of the ZnSe/GaAs (001) heterostructure. They found two resonances in the interface spectra. The one at 2.92 eV was assigned to the E_1 transition of GaAs and the stronger resonance at 2.72 eV was assigned to a virtual crossover transition connecting a resonance state of the GaAs interfacial quantum well and the ZnSe valence band. In the course of their studies, they found an interference in the reflected SHG signal from the two adjoined nonlinear slabs.[18,19]

In this article, we report on our studies using allowed and forbidden LO Raman scattering via the Fröhlich interaction as a *counterpart* to 3PM or SHG studies. Whereas Raman scattering by LO phonon involves two-photon-induced dipole transitions between electronic levels and the scattering of an electron or hole by the LO-phonon field, SHG involves the coherent interaction of three-photon-induced dipole transitions. The symmetries and selection rules for the LO Fröhlich Raman scattering resemble those of SHG since the Fröhlich matrix element can be cast into the same form as the photon field operator. Both processes are 3WM,[3,4] involving three "momentum-conserving" virtual electronic transitions which are accompanied in any time order, by the annihilation of an input photon of frequency $\omega_1=\omega_i$, the creation or annihilation of a phonon (photon) of frequency $\omega_2=\omega_l$ ($\omega_2=\omega_i$), and the creation of a photon $\omega_3=\omega_i\pm\omega_l$ ($\omega_3=2\omega_i$) in Raman scattering (SHG). The first transition involves a direct interband excitation creating an electron–hole (e–h) pair. The second transition involves either an intraband excitation (in a two-band 3WM process) or an interband excitation of the electron (or hole) in the intermediate state to a third band (in a three-band 3WM process). The third transition involves the recombination of the excited e–h pair in the second intermediate state, returning the medium to its electronic ground state.

The materials under investigation in this work, i.e., ZnSe and GaAs, have zincblende structures, and the optical phonon in this case possesses simultaneously the character of a vector and second-rank tensor. In case of interband transition occurring in the bulk of the material, the Raman LO-phonon selection rules predict that for a mode polarized and propagating along a $Z=[001]$ direction, one photon must be polarized along X [100] and the other along Y [010], i.e., the allowed LO-phonon Fröhlich interaction for cross polarization. For SHG, this would correspond to a polarization configuration p in/s out with the plane of incidence parallel to

 0734-211X/94/12(4)/2598/7/$1.00

the crystalline [100] direction, i.e., one nonzero second-order electric susceptibility bulk component $\chi^{(2)}_{xyz}$.

In the case of Raman scattering via two-band processes, Loudon[20] has shown that in the long-wavelength limit ($q_{LO}=0$), the relatively large Fröhlich interaction matrix elements for the intraband scattering of the electron and hole have the same magnitude, but opposite signs and therefore cancel. However, when q_{LO} is finite ($\neq 0$) and the electron and hole masses are unequal, the Fröhlich matrix elements for the intraband scattering of the electrons and holes do not cancel, leading under resonance conditions to a sizeable wave-vector-dependent contribution to the Raman scattering by LO phonons. The two-band Fröhlich interaction mechanism for Raman scattering by LO phonons is particularly important when the incident radiation, and therefore also the scattered radiation, is resonant with a direct energy gap as will be shown in the next section in the case of resonance scattering from ZnSe. In SHG, the corresponding two-band process via an intermediate intraband Fröhlich interaction requires an input p-polarized photon.

Furthermore, it is well known that sizeable space-charge fields may exist at semiconductor surfaces and at the interface of heterojunction systems. Such fields, which are associated with band bendings, induce a sizeable Raman scattering by LO phonons via a Franz–Keldysh two-band electric mechanism, electric-field-induced Raman scattering (EIRS).[3] In the presence of band bending, the electric-dipole-allowed interband transitions correspond to Franz–Keldysh tunneling assisted optical transitions that create "polarized" (i.e., spatially separated) excited continuum e–h pairs, or excitons. As a consequence, the Fröhlich interaction matrix elements for the intraband scattering of the excited electron and hole by the Coulomb field of the LO phonon (RS) or the p-polarized ω_2 input wave (SHG) do not cancel even in the long-wavelength limit. The strength of the intraband Fröhlich matrix elements is determined by the e–h separation in the intermediate state and therefore, by the extent of the band bending. The EIRS can only be observed for parallel polarization ($\hat{e}_i \| \hat{e}_s$) in backscattering configuration. This corresponds in SHG to $\chi^{(2)}_{zzz}$ (p in/p out) configuration.

Generally, the mechanisms giving rise to forbidden LO-phonon scattering may be either EIRS effects or wave-vector-dependent effects associated with the nonuniform surface electric field. However, it is difficult to distinguish the two effects purely on the basis of symmetry or polarization selection rules alone since both scattering processes are described by a fourth-rank tensor. Hence, only in the absence of the surface (interface) electric fields can any residual wave-vector-dependent scattering be unambiguously determined.

The lattice constants of GaAs and ZnSe at room temperature are 5.6533 and 5.6684 Å, respectively. This corresponds to a lattice mismatch of $|a(\text{GaAs})-a(\text{ZnSe})|/a(\text{GaAs}) = 0.27\%$. Because of this small lattice mismatch between ZnSe and GaAs, there exists a tetragonal distortion in the ZnSe unit cell. As a result a biaxial compressive strain is produced in the overlayer. The elastic energy associated with this elastic strain increases with increasing the thickness of the ZnSe overlayer until there is enough energy to create a misfit dislocation at the interface. This process reduces the strain at the interface, and the largest value of overlayer thickness that corresponds to a no-misfit dislocation is the critical thickness h_c. Samples with an overlayer thickness less than h_c are free from dislocations and are pseudomorphic. Furthermore, most previous Raman studies of the ZnSe/GaAs system were concerned with doped GaAs and/or ZnSe.[11–13] This normally leads to relatively large band bending at the interface, resulting in an electric potential barrier height ϕ_b and electric field E_s at the interface.

In our study, the substrate GaAs is undoped. However, it is known that Zn and Ga diffuse across the buried interface during growth with different diffusion lengths, so that relatively high dopant densities arise near the interface. Because Zn is an acceptor in GaAs and Ga is a donor in ZnSe, their diffusion produces an intrinsic band bending at the interface.[2] As a result of this band bending and energy offsets, an interfacial quantum well forms in the GaAs conduction band. The scattering intensity for interface EIRS by LO phonons, i.e., the forbidden LO Fröhlich interaction, is proportional to the square of the electric field at the interface and consequently directly proportional to the barrier height ϕ_b. This technique offers a unique possibility to measure barrier height at interfaces.[11–13] Our measurements of the EIRS spectra from ZnSe and GaAs on both sides of the heterostructure interface is a result of the band bending and associated quantum well located at the interface, which is evidence of the interdiffusion process in our samples. In addition, we also observed a clear interference effect in the allowed and, to a lesser degree, in the forbidden LO Raman signals from both ZnSe and GaAs that correspond to the interference effect found for the SHG.[18]

II. EXPERIMENT

The samples were grown at Bellcore, New Jersey by molecular beam epitaxy (MBE) in a dual-chamber Riber MBE system. The samples were of thickness that varied between 50 and 5000 Å and consist of undoped ($n \leq 1\times10^{15}$ cm^{-3}) ZnSe (001) grown on an 0.5 μm undoped ($n \leq 5\times10^{15}$ cm^{-3}) GaAs (001). The entire heterostructure was grown on an n^+ silicon-doped GaAs substrate.[21] Zn and Ga diffuse across the buried interface during the growth and the diffusion length for Ga (Zn) in ZnSe (GaAs) is about 30 Å (100 Å) so that relatively high dopant densities (4×10^{19} cm^{-3}) arise near the interface.[2]

The Raman scattering was carried out in the backscattering geometry with the incident light on the (001) surface. In one configuration, the incident and scattered photons are taken in the cross polarization required for the measurement of the allowed LO phonons with the incident and scattered radiation polarized along [100] and [010] crystallographic directions, respectively. In a second configuration, for the measurement of the EIRS and the wave-vector-dependent forbidden RS by LO phonon, both the incident and scattered radiations were in the parallel polarization, either along the (100) or the (010) direction. The exciting light used was from an Ar^+ ion laser operating at 4880 Å (2.54 eV) for measurements far from resonance for ZnSe and operating at 4579 Å (2.71 eV) for measurement close to resonance.

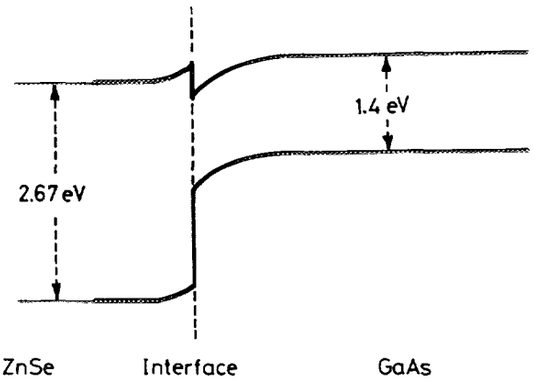

FIG. 1. Energy-band profile as a function of the depth for the ZnSe/GaAs (001) system.

All the Raman spectra reported here were taken at room temperature since low temperatures down to nitrogen temperature did not significantly change the structure of the spectrum. We used a J-Y Ramanor HG2S double monochromator with a resolution of 2 cm^{-1} and conventional photon counting electronics. A cylindrical lens was used to avoid heating the sample and to ensure lack of photoexcitation, and the intensities of the Raman line varied linearly with the incident laser radiation. Figure 1 illustrates the features for the conduction and valence band for both ZnSe and GaAs at the interface.[17]

III. RESULTS AND DISCUSSION

The results in this section are presented in two parts according to the excitation wavelength: a far-from-resonance first part, where the exciting photon, $\lambda=4880$ Å, is not absorbed by the ZnSe layer, and a near-resonance second part, where the incident photon wavelength is 4517 Å. Both regions were studied for ZnSe layers of thickness 50, 250, 650, 1000, and 1330 Å, i.e., overlayer thicknesses that are either equal to or less than the critical thickness h_c [≈1500 Å (Refs. 11–13 and 17)], and an overlayer thickness of 5000 Å.

A. Far from resonance

Figure 2 shows the first-order Raman spectra for the undoped ZnSe/GaAs (001) heterostructure for a ZnSe layer thickness $D_{ZnSe}=250$ Å in the $z(x,y)\bar{z}$ allowed configuration (curve 1) and in the $z(y,y)\bar{z}$ forbidden configuration (curve 2). In the allowed configuration, two peaks are observed: a peak appears at 292 cm^{-1} whose position agrees with the bulk LO-phonon value and is due to bulk scattering by LO-phonon modes in GaAs, and the other weaker peak observed at 256 cm^{-1} is due to bulk scattering by LO-phonon modes in ZnSe. In this $z(x,y)\bar{z}$ configuration, the deformation potential and the Fröhlich electro-optical mechanisms are the main scattering processes for both the LO_{GaAs} and the LO_{ZnSe} phonons. In the forbidden configuration, two peaks were also obtained at the same positions for the LO_{GaAs} and the LO_{ZnSe} phonons. These modes arise due to scattering at the heterointerface. It is clear from the two spectra that the allowed

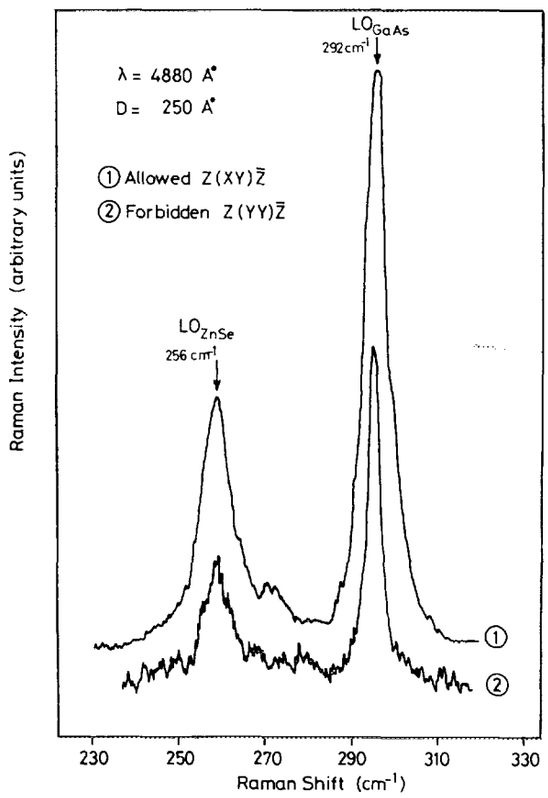

FIG. 2. First-order Raman spectra for the undoped ZnSe/GaAs (001) heterostructure obtained at $\lambda=4880$ Å for ZnSe layer thickness $D_{ZnSe}=250$ Å in the $z(xy)\bar{z}$ allowed configuration (curve 1) and in the $z(yy)\bar{z}$ forbidden configuration (curve 2).

scattering is greater than the forbidden scattering for both GaAs and ZnSe spectra. In Figs. 3(a) and 3(b), spectra, obtained for different thicknesses of ZnSe (as indicated), are given for both allowed and forbidden configurations, respectively. The thickness dependence of the Raman scattering intensity at $\lambda=4880$ Å is plotted for ZnSe in Fig. 4(a) and for GaAs in Fig. 4(b). The allowed and forbidden intensities are shown in the same figure for ease of comparison. The first striking feature of the ZnSe spectra is that the intensities of the allowed LO_{ZnSe}-phonon peaks are not varying linearly with the thickness of the ZnSe layer as would have been expected from the dependence of the Raman intensity on the length of scattering layer,[20] since this interaction is bulk generated and ZnSe is transparent at this frequency. Similar to what is observed in SHG for both the allowed LO_{ZnSe} and the allowed LO_{GaAs} scattering intensities, there is an oscillatory variation with D_{ZnSe}. Furthermore, the detected intensity for both the allowed ZnSe and GaAs spectra diminishes to the noise level for the largest available thickness $D_{ZnSe}=5000$ Å. To our knowledge, this is the first time LO Raman intensity has been observed as an oscillatory function of the thickness of overlayer. The intensities of LO_{ZnSe} peaks reported in Ref. 12 varied monotonically with thickness. Oscillatory behavior is expected to arise when the Fröhlich interaction, throughout the thickness of the ZnSe overlayer, results in an interference

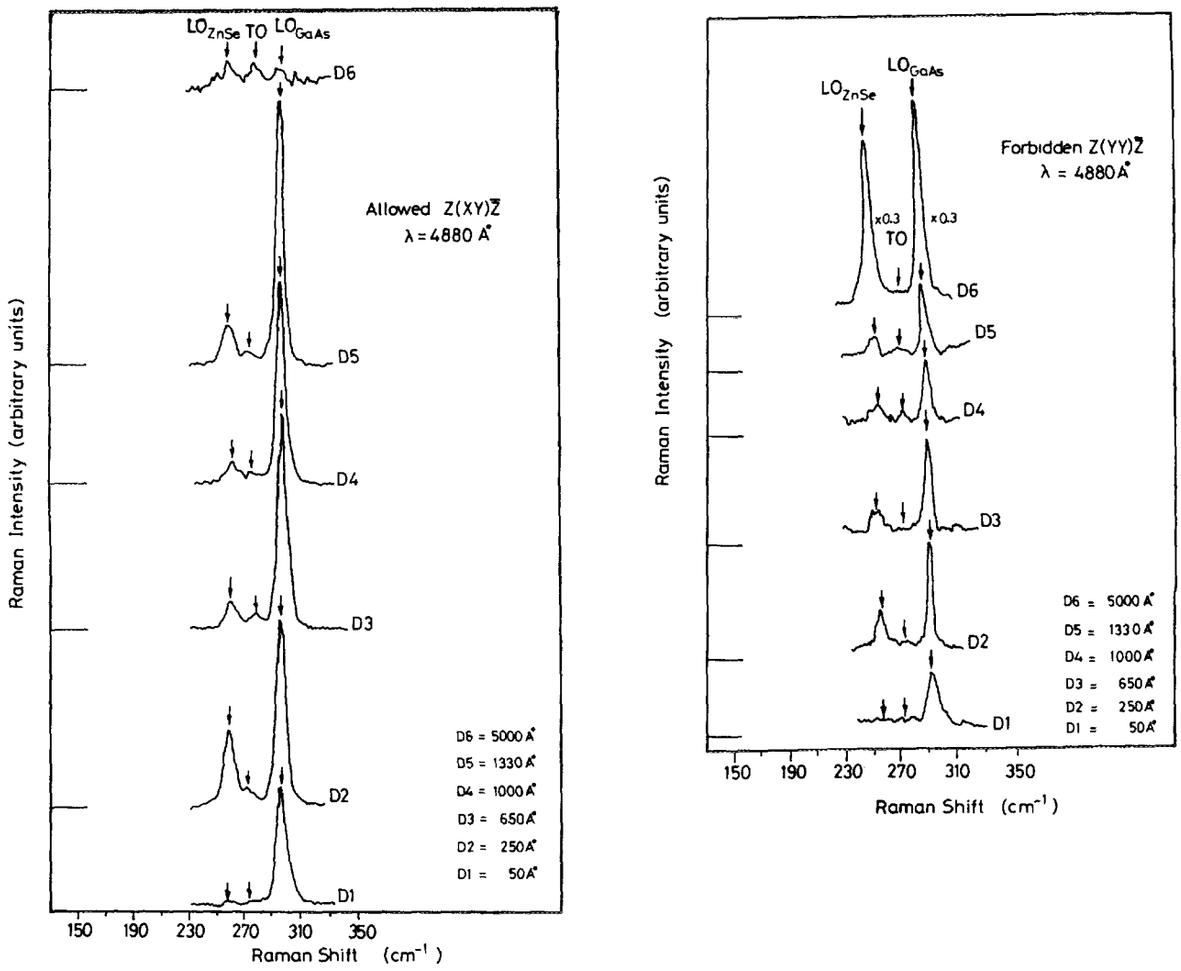

FIG. 3. (a) First-order Raman spectra for the undoped ZnSe/GaAs (001) heterostructure obtained at λ=4880 Å for different ZnSe thicknesses in the $z(xy)\bar{z}$ allowed configuration. The horizontal lines indicate the background levels and the TO_{GaAs} region is indicated. (b) First-order Raman spectra for the undoped ZnSe/GaAs (001) heterostructure obtained at λ=4880 Å for different ZnSe thicknesses in the $z(yy)\bar{z}$ forbidden configuration. The horizontal lines indicate the background levels and the TO_{GaAs} region is indicated.

effect due to reflections from both sides of the overlayer (free ZnSe and the ZnSe/GaAs interface) as shown in Fig. 5. Furthermore, the oscillation in the intensities of the LO_{GaAs} peak can also be explained in a similar fashion where in this case the interference effects manifest themselves in the transmitted EM fields through the overlayer as indicated in the figure. Since the LO_{GaAs} Raman shift is only 292 cm^{-1}, the ZnSe overlayer is nonabsorbing at the scattered frequency and acts as a Fabry–Pérot étalon in transmission.[22] The fact that, in our case, we are able to observe these variations is due to the availability of three samples less than h_c whereas, in Refs. 11 and 12, there was only one ZnSe thickness of 500 Å. This interference observation may explain the disappearance of the LO peaks in a similar system of ZnSe/GaAs [1000 Å of ZnSe deposited on (100) GaAs substrate] at a wavelength 4880 Å and their observations at 5145 Å.[23]

The variation of surface EIRS has previously been extensively applied[11–13] to characterize the heterointerface of the ZnSe/GaAs system and to determine barrier heights and their change with thickness D_{ZnSe}. These studies were mostly concerned with highly doped GaAs substrates. In our case, the GaAs substrates are undoped semi-insulating ($n \leq 5\times10^{15}$ cm^{-3}) and the observation of these forbidden LO-phonon scattering spectra is a direct evidence for the presence of band bending at the interface of these undoped ZnSe/GaAs samples. Furthermore, as can be observed in Fig. 4(b), the EIRS effects are more dominant than the wave-vector-dependent scattering at this nonresonant incident frequency. The behavior of the forbidden LO_{GaAs} is in general agreement with the observation of Olego,[11,12] i.e., low intensities in the pseudomorphic region and much larger intensities as the overlayer increased beyond h_c, due to misfit dislocations and a larger interface electric field. From Figs. 4(a) and 4(b) the variation observed in the intensities of the forbidden LO-phonon scattering for ZnSe and GaAs in the pseudomorphic region of the overlayer is much smaller than in the allowed case. This is due to the relatively small surface fields in these pseudomorphic regions, resulting in small scattering intensi-

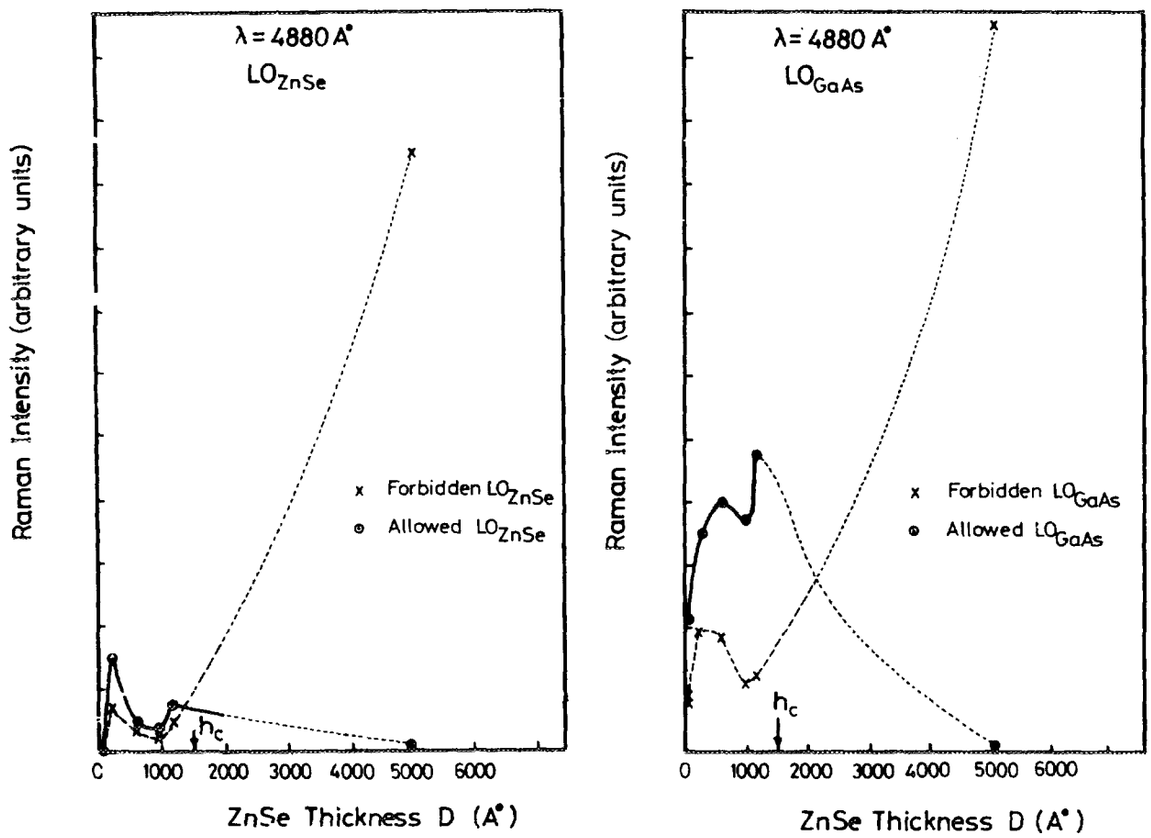

FIG. 4. Thickness dependence of (a) the LO_{ZnSe} and (b) the LO_{GaAs} Raman scattering intensity at λ=4880 Å. Allowed and forbidden intensities are shown in the same figure for ease of comparison. The critical thickness h_c above which misfit dislocations are present at the interface is indicated in the figure. The dashed lines between $D_{ZnSe}=h_c$ and 5000 Å were drawn as visual aids.

ties and less effective interference effects. Unfortunately, most of our samples were in the pseudomorphic region, and we did not have access to samples with thicknesses between 1330 and 5000 Å; therefore we were unable to follow these variations more precisely in the region $D_{ZnSe}>h_c$.

B. Near resonance

Figures 6(a) and 6(b) show the scattered allowed and forbidden LO Raman spectra obtained at λ=4579 Å for different ZnSe thicknesses in the two scattering configurations, $z(x,y)\bar{z}$ and $z(y,y)\bar{z}$, respectively. In these figures, the

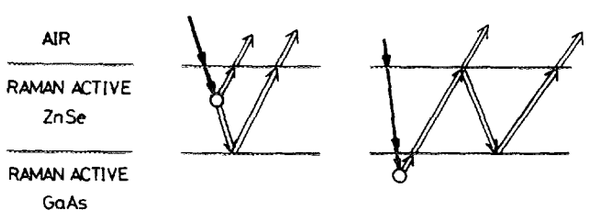

FIG. 5. Geometry used to explain the Raman LO radiation inside the epitaxial ZnSe overlayer and the GaAs substrate ($\rightarrow\omega_i\Rightarrow\omega_i-\omega_L$).

$2LO_{ZnSe}$ peaks, which are much weaker, are also shown. However, the 2LO spectra has approximately the same shape as the 1LO indicating that only the phonons from the center of the Brillouin zone are contributing to the scattering. In Fig. 6(a), the observed allowed Fröhlich intensity is due to the bulk interaction in the penetration depth δ (≈2600 Å), and hence for overlayers of thickness $D_{ZnSe}<\delta$, interference oscillatory behavior could also be detected (as in the case of the off resonance). This can be seen in Fig. 7 for thickness less than h_c. The noncancellation of the peak for the thickness D_{ZnSe}=5000 Å, is due to the fact that the interaction is through the skin depth only, and the fields are not uniform over the whole thickness of the overlayer and hence the interference conditions are not realized. It is evident from the enhanced intensity of the forbidden LO-phonon scattering shown in Fig. 6(b) that, in addition to the EIRS scattering, the dominant wave-vector-dependent effects due to intraband scattering appear at resonance in this diagonal configuration for LO_{ZnSe}. The intensity of the forbidden scattering also shows the interference oscillatory behavior but is an order of magnitude larger than the allowed LO_{ZnSe}-phonon scattering (see Fig. 7). Furthermore, the forbidden LO wave-vector-dependent scattering is also larger than the 2LO-phonon scattering, which is allowed in this configuration. In off reso-

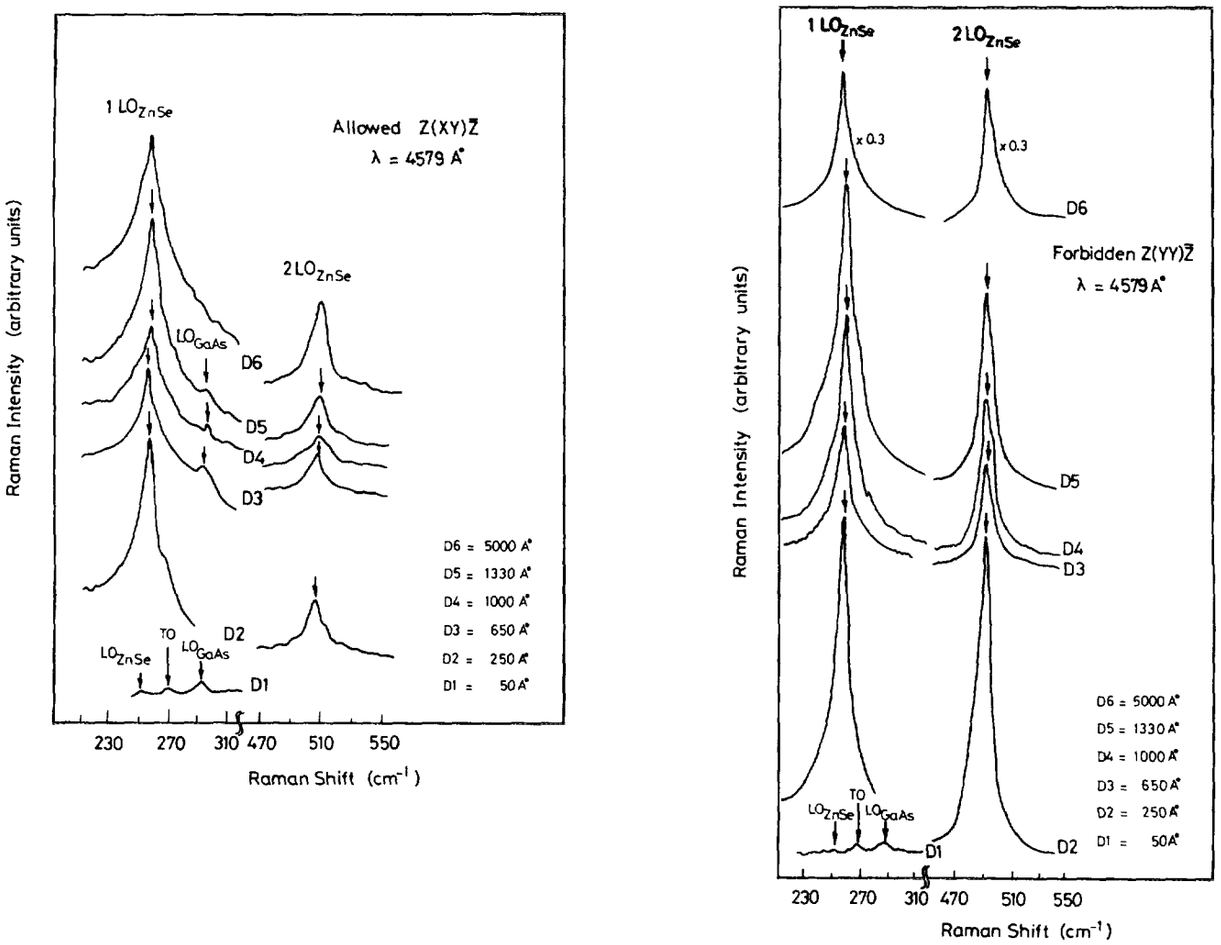

FIG. 6. Scattered Raman spectra obtained at λ=4579 Å for different ZnSe thicknesses in the (a) allowed configuration and (b) forbidden configuration.

nance, $2LO_{ZnSe}$ phonons were barely detectable for the used incident power and our sensitivity; as resonance is approached, the $2LO_{ZnSe}$ scattering efficiency grows, indicating that the Frohlich interaction is strong.

In this forbidden configuration, as mentioned before, it is difficult to separate the wave-vector-dependent LO_{ZnSe} scattering from the EIRS on the basis of symmetry and polarization alone. However, the EIRS effects get weaker as the band bending gets smaller (D_{ZnSe} increases towards h_c), and the contribution of the wave-vector-dependent Fröhlich interactions increases as the incident photon energy approaches the band gap. Then, for the near-resonance incident frequency, in the region of $D_{ZnSe} \cong h_c$ where the bands are almost flat at the interface, and the skin depth is at least twice the thickness of the overlayer, the difference in the intensity of the forbidden LO-phonon scattering from the allowed configuration is then a measure of the wave-vector-dependence enhancement. This enhancement continues to show in the thicker sample (D_{ZnSe}=5000 Å) where a crossover transition would be buried at twice the penetration depth, indicating that such a crossover transition has no contribution to this enhancement. This is also evident in the pseudomorphic region where no enhancement in the forbidden LO-phonon scattering intensity for GaAs, due to such a crossover transition, was observed.

Experiments on photomodulation of the bands at the interface to separate the EIRS from other contributions due to wave-vector-dependent enhancement by achieving flat-band conditions in each material separately are now underway and will be reported in a forthcoming publication. It is to be noted that, unlike 3PM, where $\omega_1+\omega_2=\omega_3$ are independent of spatial region, Fröhlich LO Raman scattering can yield the fingerprint of the medium in which it occurs as well as the different spatial regions (i.e. surface, interface quantum well or substrate) and the specific processes (e.g., plasmon coupling, etc.) that are involved. We may further remark that the resonant two-band RS corresponds to double resonance leading to a strong enhancement, whereas SHG using a single input beam can exhibit only a single resonance either at the input or at the output frequency. However, there is a greater attenuation for RS at resonance due to absorption in ZnSe proportional to $e^{-\alpha D_{ZnSe}}$ and an enhancement factor which is proportional to $(E_{res}-\hbar\omega-\gamma)^{-2}$; hence the ratio of the scattered intensities for RS to SHG is proportional to $e^{-\alpha D_{ZnSe}}(E_{res}-\hbar\omega-\gamma)^{-1}$. This enhancement facilitates LO Raman studies of buried interfaces.

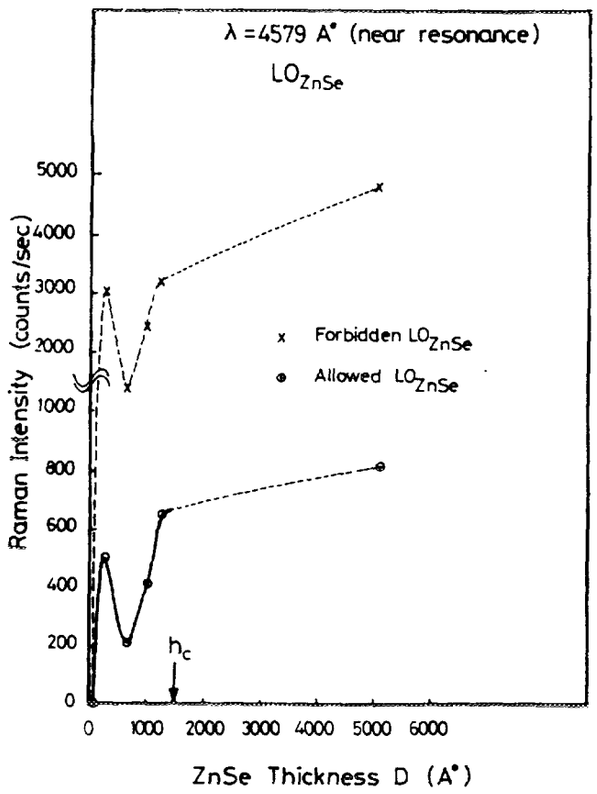

FIG. 7. Thickness dependence of the LO_{ZnSe} Raman scattering at $\lambda = 4579$ Å (near resonance). Allowed and forbidden intensities are shown in the same figure for ease of comparison. The critical thickness h_c above which misfit dislocations are present at the interface is indicated in the figure. The dashed lines between $D_{ZnSe} = h_c$ and 5000 Å were drawn as visual aids.

IV. CONCLUSION

We have applied the Fröhlich LO interaction as the counterpart to SHG to study the heterostructure interface of ZnSe/GaAs. At nonresonant incident frequencies (in ZnSe), the forbidden LO_{GaAs} intensities show variations with D_{ZnSe}. In the allowed configuration, we have observed a clear interference effect in the intensities of LO_{ZnSe} as well as for LO_{GaAs}. These interference effects are similar to interference effects observed recently in nonlinear second harmonic generation for identical ZnSe/GaAs heterostructures.[18] At a ZnSe resonant incident frequency, the forbidden LO-phonon scattering shows strong enhancement due to wave-vector-dependent scattering and EIRS; however, enhancement due to wave-vector dependence can be separated from EIRS at the critical thickness where the bands are flat.

ACKNOWLEDGMENT

The authors gratefully acknowledge Dr. M. Tamargo for providing them with the samples.

[1]K. Mohammed, D. A. Cammack, R. Dalby, P. Newbury, B. L. Greenberg, J. Petruzzello, and R. N. Bhargava, Appl. Phys. Lett. **50**, 1 (1987).
[2]L. Kassel, H. Abad, J. W. Garland, P. M. Raccah, J. E. Potts, M. A. Haase, and H. Cheng, Appl. Phys. Lett. **56**, 42 (1990).
[3]E. Burstein, G. Pajer, and A. Pinczuk, *Proceedings of the International Conference on the Physics of Semiconductors*, Stockholm, 1986, edited by O. Engstrom (World Scientific, Singapore, 1987), p. 1691.
[4]E. Burstein and M. Y. Jiang, in *Light Scattering in Semiconductor Structures and Superlattices*, edited by D. J. Lockwood and J. F. Young (Plenum, New York, 1991), p. 441.
[5]J. F. McGilp and Y. Yeh, Solid State Commun. **59**, 91 (1986).
[6]T. F. Heinz, F. J. Himpsel, E. Palange, and E. Burstein, Phys. Rev. Lett. **63**, 644 (1989).
[7]E. Gharhrmani, D. J. Moss, and J. E. Sipe, Phys. Rev. Lett. **64**, 2815 (1990).
[8]M. S. Yeganeh, A. G. Yodh, and M. C. Tamargo, in *Quantum Electronics Laser Science*, 1991 Conference Edition (Optical Society of America, Washington D. C., 1991), p. 30; J. C. Hamilton, R. T. Tung, and H. W. K. Tom, *ibid.*
[9]E. Burstein and A. Pinczuk, in *The Physics of Opto-Electronic Materials*, edited by Walter A. Albers, Jr. (Plenum, New York, 1971), p. 33.
[10]J. G. Gay, J. D. Dow, E. Burstein, and A. Pinczuk, in *Proceedings of the Second International Conference on Light Scattering in Solids*, edited by M. Balkanski (Flammarion, Paris, 1971), p. 33.
[11]G. Abstreiter, E. Bauser, A. Fisher, and K. Ploog, Appl. Phys. **16**, 345 (1978).
[12]D. J. Olego, Appl. Phys. Lett. **51**, 18 (1987).
[13]D. J. Olego, J. Vac. Sci. Technol. B **6**, 4 (1988).
[14]D. J. Olego, Phys. Rev. B **39**, N17 (1989).
[15]O. Brafman, J. Vac. Sci. Technol. B **10**, 4 (1992).
[16]A. Krost, W. Richter, D. R. T. Zahn, K. Hingert, and H. Sitter, Appl. Phys. Lett. **57**, 19 (1990).
[17]M. S. Yeganeh, J. Qi, A. G. Yodh, and M. C. Tamargo, Phys. Rev. Lett. **68**, 3761 (1992).
[18]M. S. Yeganeh, J. Qi, J. P. Culver, A. J. Yodh, and M. C. Tamargo, Phys. Rev. B **46**, 1603 (1992).
[19]An interference enhanced Raman spectra was used to study very thin evaporated films of metallic titanium and oxidized titanium; R. J. Nemanich, C. C. Tsai, and G. A. N. Connell, Phys. Rev. Lett. **44**, 273 (1980).
[20]R. Loudon, Proc. R. Soc. London Ser. A **275**, 218 (1963).
[21]M. C. Tamargo, R. E. Nahori, B. J. Skromme, S. M. Shibli, A. L. Weaver, R. J. Martin, and H. H. Farrell, J. Cryst. Growth **111**, 741 (1991).
[22]G. Hernandez, *Fabry-Pérot Interferometry*, Cambridge Studies in Modern Optics, (Cambridge University Press, Cambridge, 1986).
[23]L. Kassel, J. W. Garland, P. M. Raccah, M. Tamargo, and H. H. Farrell, Semicond. Sci. Technol. A **6**, 152 (1991).